The Journal of Physical Chemistry Letters

Letter

Structures of Ionic Liquid Having both Anionic and Cationic Octyl Tails: Lamellar Vacuum Interface vs. Sponge-Like Bulk Order

Weththasinghage Don Amith, Jeevapani J. Hettige, Edward W. Castner, and Claudio Javier Margulis

J. Phys. Chem. Lett., **Just Accepted Manuscript** • DOI: 10.1021/acs.jpclett.6b01763 • Publication Date (Web): 08 Sep 2016

ACS Publications

The Journal of Physical Chemistry Letters is published by the American Chemical Society. 1155 Sixteenth Street N.W., Washington, DC 20036

Structures of Ionic Liquid having both Anionic and Cationic Octyl Tails: Lamellar Vacuum Interface vs. Sponge-Like Bulk Order

Weththasinghage Don Amith[†], *Jeevapani J. Hettige*[†], *Edward W. Castner Jr.*[‡] *and Claudio J. Margulis*[†*]

[†]Department of Chemistry, University of Iowa, Iowa City, Iowa 52242, United States

[‡]Department of Chemistry and Chemical Biology, Rutgers, The State University of New Jersey, Piscataway, New Jersey 08854, United States

AUTHOR INFORMATION

Corresponding Author

*Email: claudio-margulis@uiowa.edu

ABSTRACT: Numerous experimental and computational studies have shown that the structure of ionic liquids is significantly influenced by confinement and by interactions with interfaces. The nature of the interface can affect the immediate ordering of cations and anions changing important rheological characteristics relevant to lubrication. Most studies suggest that such changes are local or short ranged and that bulk properties are reestablished on a length scale of a few nanometers. The current study focuses on the 1-methyl-3-octylimidazolium octylsulfate ionic liquid for which both the cation and anion have moderate length linear alkyl tails. For this system we find that the bulk phase is dominated by the very common sponge-like morphology characteristic of many ionic liquids. However, at the vacuum interface a lamella structure is observed that is not restricted to the vicinity of the surface but instead extends across the full 9 nm slab of our simulation. We suspect that in reality it could extend significantly beyond this.

TOC GRAPHICS

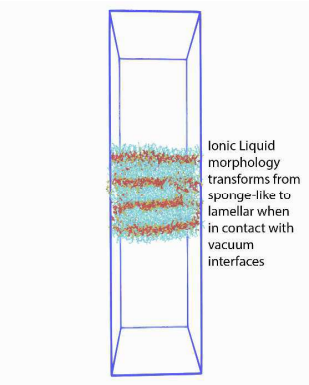

KEYWORDS Ionic Liquid, Phase Transition, Confinement, Long Range Transformations, Surfaces, Interfaces.

There is already extensive literature on the interaction of ionic liquids (ILs) with surfaces and in confined environments[1-31]. Recent review and perspective articles by the groups of Atkin, Greaves and Salanne provide interesting and enlightening standpoints on different aspects of ionic liquids at interfaces.[3,32-34] However, very recently several experimental studies[35-37] (also Welton, T. ASIL7 - 7th Australian Symposium on Ionic Liquids, 2016) have challenged our most basic understanding of ILs based on well conducted simulations for systems with interfaces. These experiments appear to imply that interaction with surfaces can induce phenomena that are much longer ranged and that persist for much longer times than would be expected from simulation results. Because of charge screening, simulations would often predict that effects of interfaces should decay within a couple of nanometers. Furthermore, establishing ionic gradients on these length scales should occur on computationally accessible time scales of nanoseconds. An intriguing recent article by the group of Espinosa-Marzal[35] demonstrated that the use of an extended surface force apparatus that repeatedly imposes and releases confinement of a film of 1-hexyl-3-methyl-imidazolium ethylsulfate, induces a phase transformation that was not relieved by the removal of such confinement; the induced structure extended over 60 nm, a length scale over which surface properties would be expected to dissipate. Another interesting very recent experiment reported by Shaw and coworkers[36] was an order-disorder transition over a micrometer length scale when IL films based on the TFSI anion were formed while applying shear. Relaxation of this order occurred only on a time scale of hours. Yet another study by the group of Haverhals[37] where cyclic voltammetry coupled with surface enhanced infrared absorption spectroscopy was used, demonstrated that for certain ILs there appears to be hysteresis in the current-voltage curve indicating morphological changes of the IL that remain active on macroscopic time scales.

These transformations which would appear to occur on macroscopic time scales are a significant challenge for computational studies and therefore *in silico* interpretation of many of these studies is still missing. The current study focuses on the 1-methyl-3-octylimidazolium octylsulfate (C[8]-mim$^+$/C[8]-O-SO$_3^-$) system which belongs to the same family as that studied by Espinosa-Marzal but where both the anion and cation have longer octyl tails. It is expected that this increase in symmetry may facilitate the observation of order transitions that may be frustrated and difficult to observe on computational time scales for more asymmetric ions. The current work will serve as a benchmark for our experimental studies of the interfacial structure for this system using angle-resolved X-ray photoelectron spectroscopy (AR-XPS)[38-46], since AR-XPS can provide depth profiling of the atomic composition of the top 1.0-1.5 nm of the interface. AR-XPS will be able to confirm whether an excess of alkyl groups is found at the vacuum interface, though X-ray or neutron reflectivity experiments, AFM images, or other methods will be required to prove the existence of the lamellar structures we report below. The computational work presented here contains the analysis of the structure of this system in the bulk phase, with particular emphasis on a detailed study of the structure function S(q) and its subcomponents. It also contains the effect that introducing vacuum interfaces at opposite ends of a large simulation box has on liquid morphology. We will show that this perturbation results in dramatic changes that not only affect the immediate vicinity of the liquid-vacuum interface but that propagates throughout the whole simulation slab.

ILs are often composed of cations and anions of significantly different size. This is not the case for C[8]-mim$^+$/C[8]-O-SO$_3^-$ (see Fig. 1) where both species have charge heads and alkyl tails of equivalent and moderate lengths.

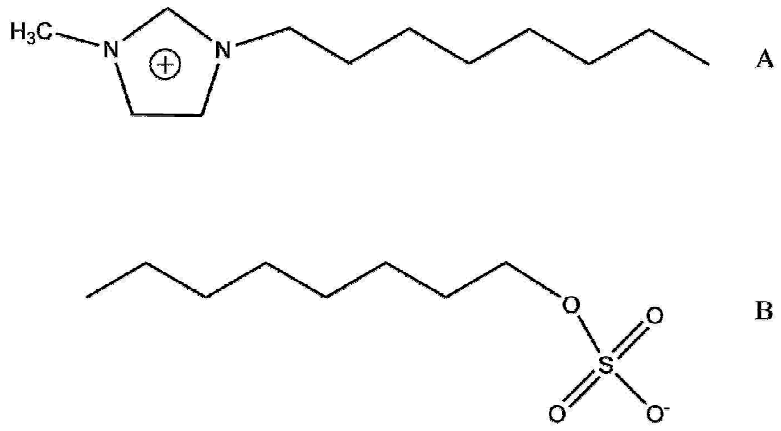

Figure 1. A = C[8]-mim+ (cation), B = C[8]-O-SO3- (anion).

In the bulk liquid phase, this structural symmetry results in a disordered but continuously percolating network of charges with alkyl tails acting as spacers between strings of alternating charge. It is expected as we have observed in prior work[47] that because positive and negative charges alternate, so should cationic and anionic alkyl tails. A three dimensional view of the system presented in Fig. 2 reveals a sponge-like structure that is reminiscent of many other previously reported in the literature.[47-50]

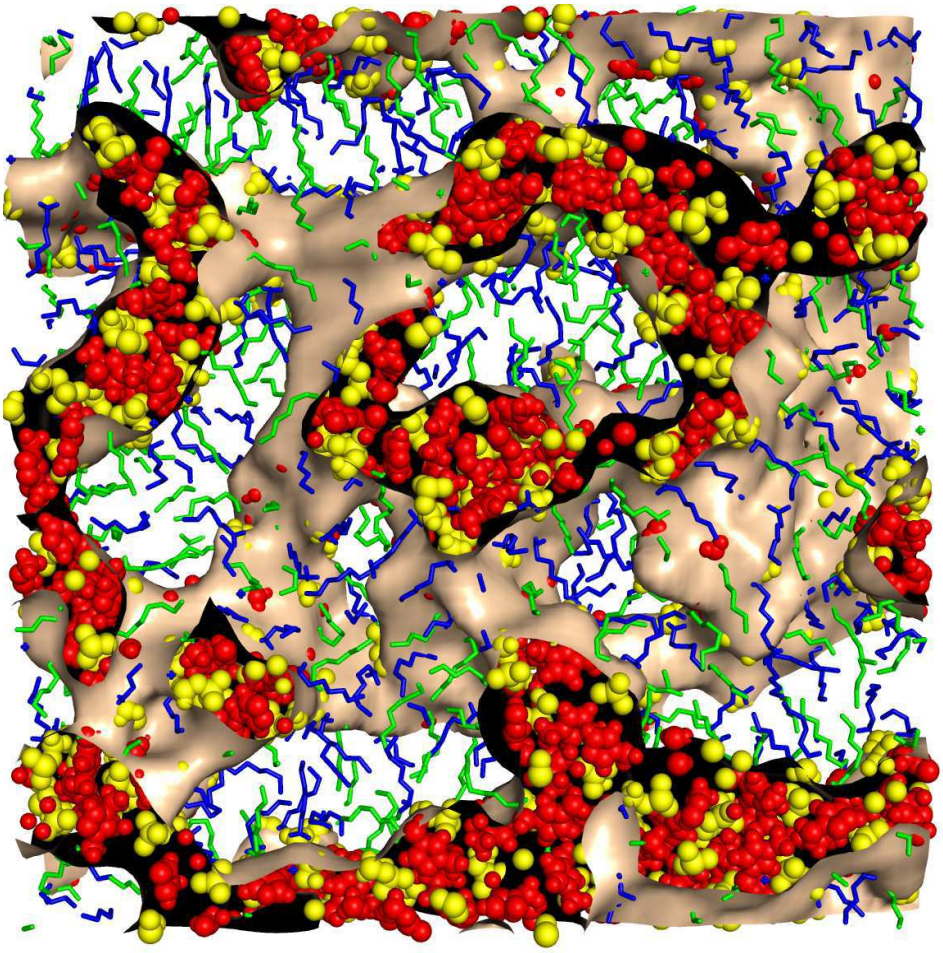

Figure 2. Snapshot of the equilibrated bulk C[8]-mim+/C[8]-O-SO3- system with surface encompassing a disordered but continuously percolating network of charges. Charge strings and apolar subcomponents appear to form a bicontinuous sponge-like pattern. (Blue-Anion tail, Green-Cation tail, Red-Cation head and Yellow-Anion head).

Figure 3 shows that the total S(q) of the bulk liquid includes the three typical features that are the hallmark of charge and polarity alternation.[47,51-58] The prepeak, associated with the typical length scale in which strings of charge are separated from other strings of charge by an apolar region can be seen at about 0.25 $Å^{-1}$, whereas a shoulder corresponding to positive-negative alternation is observed at distances slightly below 1 $Å^{-1}$. The peak at around 1.4 $Å^{-1}$ is associated with all types of intramolecular and short range intermolecular interactions between adjacent species.

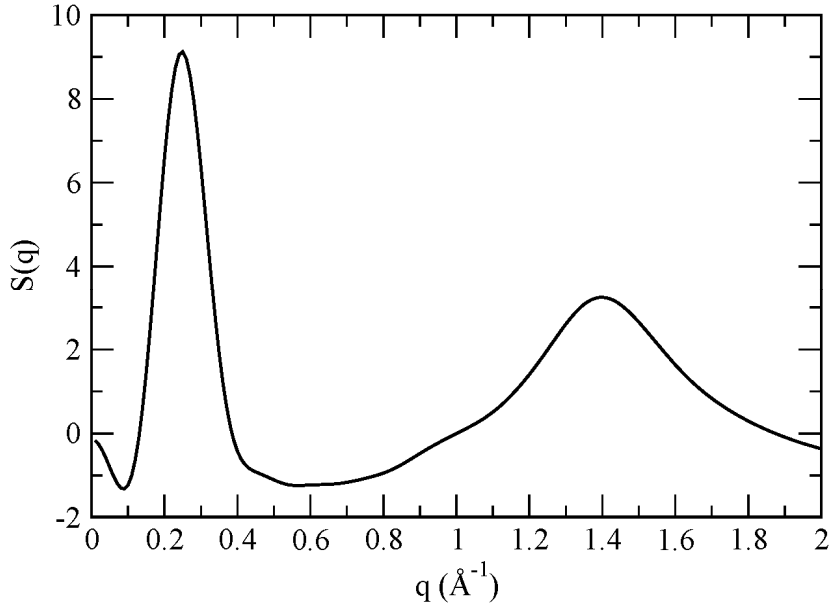

Figure 3. Computationally derived total structure function S(q) for the equilibrated bulk IL.

A noticeable feature in Fig. 3 is that the prepeak appears at inverse distances (q) shorter than that for most common ionic liquids, which means that this feature appears at larger length scales ($d=2\pi/q$, where d is the real space distance). This is likely a consequence of the fact that both cations and anions possess moderate size alkyl tails, whereas for most other systems only one of the species has significant apolar components. Figures 4 and 5 display subcomponents of S(q) that correspond to what we have termed natural variables.[52]

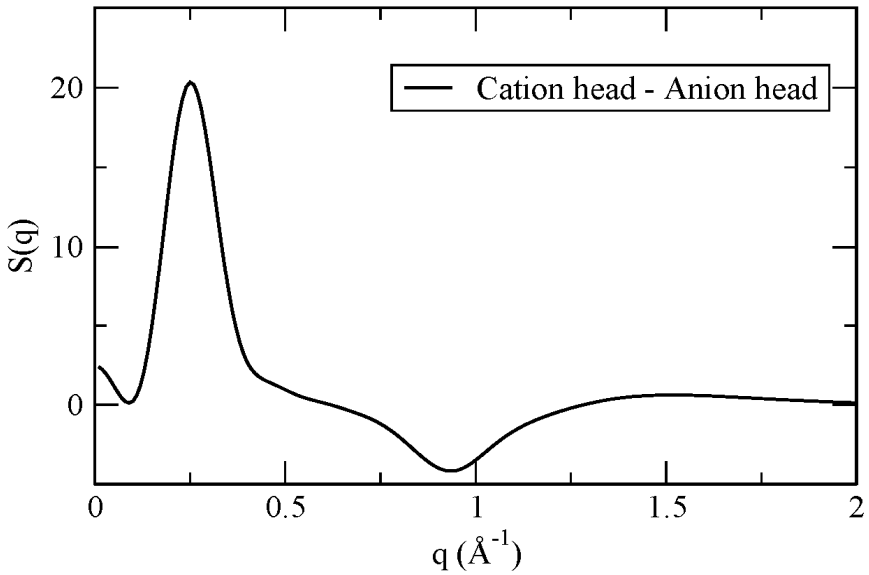

Figure 4. Partial cation-head/anion-head subcomponent of S(q) in the bulk indicating as an antipeak (at slightly less than 1 Å^{-1}) the characteristic inverse length scale associated with charge alternation and as a peak at about 0.25 Å^{-1} the characteristic inverse range for polarity alternation.

These subcomponents allow for the unequivocal interpretation of the S(q) data. The polarity partitioning of S(q) showing two peaks and one antipeak[56] at the same q value as the prepeak is indicative of the characteristic distance for polar-apolar alternation (see Fig. 5). This alternation is associated with string of charges separated by tails (or tail regions separated by strings of charge within the sponge). Instead, the charge partitioning of S(q) (of which only the cation head-anion head subcomponent is shown in Fig. 4) is useful in identifying the characteristic distance for charge alternation within network strings. The cation head-anion head subcomponent of S(q) (shown in Fig. 4) features what we have termed an antipeak at the inverse distance corresponding to charge alternation (positive and negative count as "opposite type" species in this regime)[53] whereas it displays a peak in the low q region associated with the prepeak (in this case both positive and negative charge components count as "same type" species since they are both polar).[59] This function allows for the clearest identification of the two

different alternation regimes associated with (1) polar and apolar subcomponents at low q and (2) positive and negative subcomponents in the vicinity of the q=1 $Å^{-1}$.

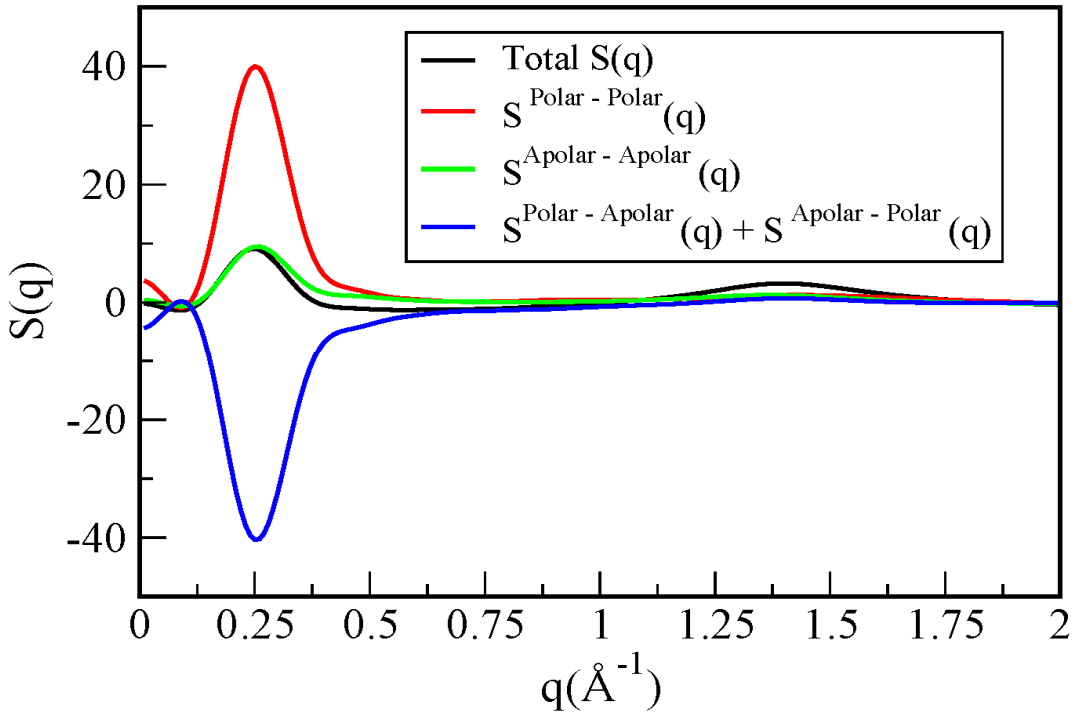

Figure 5. Total S(q) in the bulk phase and its subcomponents defined via the polarity partitioning. Two peaks (polar-polar and apolar-apolar) counter an antipeak (polar-apolar + apolar-polar) clearly identifying the periodic repetition of strings of alternating charges spaced by the apolar network. Alternatively, this also represents the typical separation between apolar subcomponents that are alternated by a polar string.

Apart from the prepeak appearing at lower q values than in most other ILs, the structure of C[8]-mim^+/C[8]-O-SO_3^- appears similar to that of many other systems we have already studied[47,51-58,60,61] where networks of polar and apolar subcomponents are present. However, what we find most interesting is the transformation that occurs upon the introduction of opposing apolar interfaces, in our case vacuum, leaving the previously equilibrated liquid in a slab configuration.

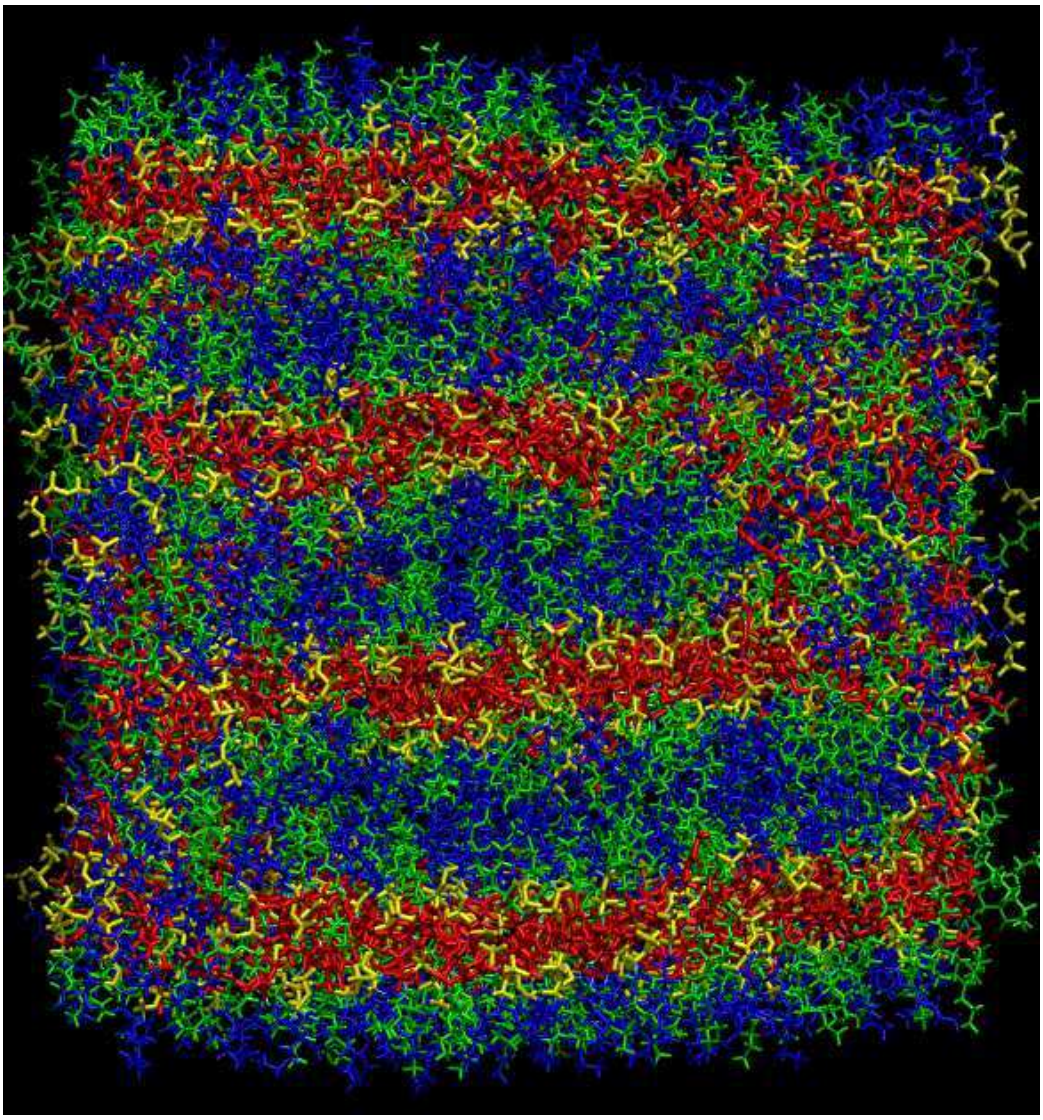

Figure 6. Snapshot of the equilibrated system in the slab conformation clearly showing C[8]-mim$^+$/C[8]-O-SO$_3^-$ in the lamellar phase. (Blue-Anion tail, Green-Cation tail, Red-Cation head and Yellow-Anion head).

Because we are interested in understanding phenomena beyond the first nanometer from the surface, we prepared a large box with 1000 ion pairs with initial configuration derived from the fully equilibrated bulk structure. The approximate distance between the two vacuum surfaces is 9 nm. Figure 6 shows that after thorough equilibration in the slab configuration the condensed phase sponge-like structure morphed into a lamellar phase. The lamellar structure was not just at the interface but instead was established across the entire slab. We expect that such phase could persist also on thicker slabs not easily accessible computationally.

Figure 7 shows the molecular number density per unit volume for cation head, cation tail, anion head and anion tail across the slab.

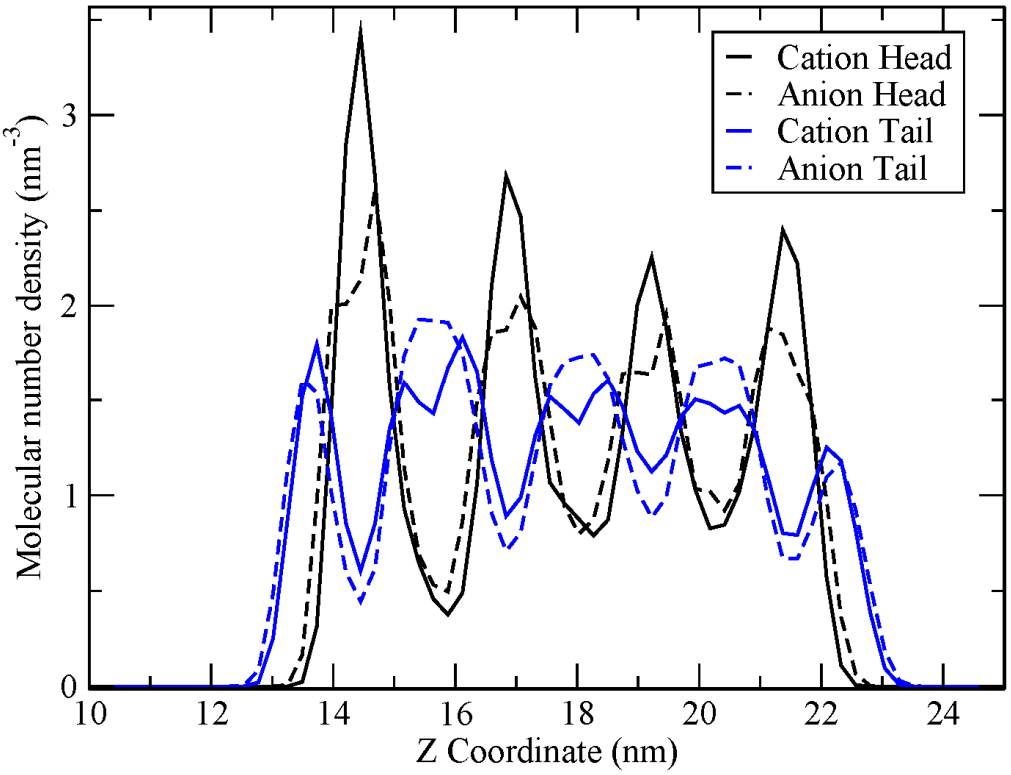

Figure 7. Molecular number density profiles for C[8]-mim$^+$/C[8]-O-SO$_3^-$ in the slab configuration. Each line represents the group or molecular number density per unit volume for different groups in the system along the Z axis of the extended simulation box.

From this we learn that cationic and anionic heads and tails oscillate in sync along the direction perpendicular to the surface. Figure S.1 in the Supporting Information, which displays the average of the first Legendre polynomial $P_1(\theta)$ across the slab, helps shed light on the nature of charge and polarity alternation in the lamellar phase. At each interface, cationic and anionic tails are vacuum exposed and inside the slab heads and tails alternate establishing the lamellar phase.

In conclusion, recent experimental observations have led to the suggestion that interactions with interfaces, electrical potentials or even certain mechanical perturbations can result in IL behavior that cannot be simply explained by polarization or close range effects of the confining interface.

The phenomena observed appear to occur on length scales and time scales much longer than would be predicted by nanometer range organization. While the data is not sufficient for an overall picture we speculate about possibilities for longer range structures induced by the interface. Can different condensed phase polymorphic phases of ILs be "engineered" on the many nanometer length scale via confinement perturbations or other external stimuli? We cannot unequivocally address this question computationally for ILs of low symmetry as time scales and length scales may be prohibitive; however, recent experiments appear to point in this direction. We emphasize that --albeit with higher symmetry-- C[8]-mim$^+$/C[8]-O-SO$_3^-$ shares significant similarities to C[6]-mim$^+$/C[2]-O-SO$_3^-$, an IL for which successive confinement interactions resulted in a disordered to ordered transformation on a 60 nm length scale that persisted on macroscopic time scales after removal of the perturbation. Hence, the current study provides a platform for the discussion and exploration of such type of longer range transformations on a time scale amenable to simulation. Our study indicates that C[8]-mim$^+$/C[8]-O-SO$_3^-$ shows a transformation from a sponge-like to a lamella phase as it comes into contact with apolar vacuum interfaces. The changes observed are not confined to the proximity of the interface but instead propagate on a 9 nm length-scale. We suspect that the system could support layered structures even thicker across hydrophobic interfaces but confirmation will require further studies. Because of the extra symmetry in our system, the sponge to lamella transformation was facile. However, other systems that are less symmetric may require macroscopic time scales for morphology changes to be observed. Such structural transformations may be much less dramatic than those observed here but may explain for example the changes in the IR spectra upon film formation in the experiments of the Shaw group. The current work does not attempt to directly address the several novel experimental observations that could potentially be consistent with longer range

transformations at interfaces with ILs. We instead provide a simple model system of an IL that at least computationally may show a many nanometer transformation upon the introduction of surface interactions. We plan in the future to study variations of this system for different alkyl tail sizes as well as other slab configurations to see if thicker lamellar phases can be supported. We hope that this work can foster further discussions, calculations and experiments that can fully elucidate these very intriguing phenomena.

Computational Methods

Bulk IL simulations: The bulk phase of 1-methyl-3-octylimidazolium octylsulfate was modeled using a simulation box containing 1000 ion pairs. All molecular dynamics (MD) runs were carried out using the GROMACS[62,63] package. Canongia Lopes-Pádua[64] and Optimized Potentials for Liquid Simulations All-Atoms (OPLS-AA)[65,66] force fields were used to model the system. As in previous studies[52,54,55,58,59,67,68] we have used several factors not just the temperature as equilibration parameters. In particular, for this study the system was equilibrated for ~ 1 ns by scaling the atomic charges from 0% to 100%, and raising and lowering the pressure. The procedure was then followed by a 4 ns simulated annealing scheme. In the annealing protocol, the temperature of the system was ramped up from 300 K to 500 K and then brought down to the desired 425 K temperature and 1 bar pressure. The equilibration was then continued for 8 ns in the NPT ensemble. The coordinates of atoms during the production run (final 1 ns) of this NPT simulation were saved every 1 ps for analysis. The temperature of the system was controlled by a Nosé-Hoover thermostat[69,70] and the pressure using the Parrinello-Rahman[71] barostat. The equations of motion were integrated using the Leap-Frog algorithm with a time step of 1 fs. Coulomb and Lennard-Jones cut-offs were set to 1.5 nm and the Particle Mesh Ewald (PME)[72,73] (EW3D) method with an interpolation order of 6 and Fourier grid

spacing of 0.8 Å was used to account for electrostatic interactions. The final dimensions of the well equilibrated simulation box were 8.95456 nm x 8.95456 nm x 8.95456 nm.

Vacuum-IL simulation: For the IL in the slab configuration, electrostatic interactions were computed by using the PME technique together with the Yeh-Berkowitz correction[74] (EW3DC). Prior to introducing the vacuum interfaces, the well equilibrated simulation box from the bulk study was further extended in the NVT ensemble for 5 ns. The last configuration was then placed at the center of a tetragonal supercell of dimensions 8.95456 nm x 8.95456 nm x 35.81824 nm so that the length of the additional empty space was larger than the lateral box lengths. This has been reported as relevant to the successful application of EW3DC.[74,75] For the initial equilibration of the slab configuration a 8 ns simulated annealing protocol was followed in which the system started 300 K above target temperature and was brought to 425 K. After this, the system was thoroughly equilibrated for more than 0.1μs at 425 K. The final 16 ns were used for the analysis of the vacuum-IL interface.

Structure Function: The structure function S(q) for the bulk IL was computed using the same formulation as in our prior studies (see for example equation 1 in reference[60]). In the current work we use the polarity partition of S(q)[59] as well as the cationic head- anionic head subcomponents of the total S(q).[53] These functions result in the most natural way[52] to analyze the features in the overall S(q) of ILs. Cation and anion head groups define the polar subcomponent; alkyl tails are the apolar subcomponent. The cationic head group is defined as the ring, the methyl group and up to the second CH_2 group in the octyl chain. The anionic head group is defined to include up to the first CH_2 group in the alkyl chain. These definitions are based on the partial charges assigned to groups in the force field.

ACKNOWLEDGMENTS

This work was supported by Grant No. CHE-1362129 from the US National Science Foundation awarded to C.J.M. and No. CHE-1362272 to E.W.C. We thank Prof. Juan Carlos Araque and Dr. Kamal Dhungana for instructive discussions as well as help rendering Fig. 2.

REFERENCES

(1) Paredes, X.; Fernández, J.; Pádua, A. A. H.; Malfreyt, P.; Malberg, F.; Kirchner, B.; Pensado, A. S. Using Molecular Simulation to Understand the Structure of [C2C1im]+– Alkylsulfate Ionic Liquids: Bulk and Liquid–Vapor Interfaces. *J. Phys. Chem. B* **2012**, *116*, 14159-14170.

(2) Konieczny, J. K.; Szefczyk, B. Structure of Alkylimidazolium-Based Ionic Liquids at the Interface with Vacuum and Water—A Molecular Dynamics Study. *J. Phys. Chem. B* **2015**, *119*, 3795-3807.

(3) Hayes, R.; Warr, G. G.; Atkin, R. Structure and Nanostructure in Ionic Liquids. *Chem. Rev.* **2015**, *115*, 6357-6426.

(4) Sarangi, S. S.; Raju, S. G.; Balasubramanian, S. Molecular dynamics simulations of ionic liquid-vapour interfaces: effect of cation symmetry on structure at the interface. *Phys. Chem. Chem. Phys.* **2011**, *13*, 2714-2722.

(5) Antelmi, D. A.; Kékicheff, P.; Richetti, P. The Confinement-Induced Sponge to Lamellar Phase Transition. *Langmuir* **1999**, *15*, 7774-7788.

(6) Sieffert, N.; Wipff, G. Ordering of Imidazolium-Based Ionic Liquids at the α-Quartz(001) Surface: A Molecular Dynamics Study. *J. Phys. Chem. C* **2008**, *112*, 19590-19603.

(7) Atkin, R.; Warr, G. G. Structure in Confined Room-Temperature Ionic Liquids. *J. Phys. Chem. C* **2007**, *111*, 5162-5168.

(8) Coasne, B.; Viau, L.; Vioux, A. Loading-Controlled Stiffening in Nanoconfined Ionic Liquids. *J. Phys. Chem. Lett* **2011**, *2*, 1150-1154.

(9) Pensado, A. S.; Gomes, M. F. C.; Lopes, J. N. C.; Malfreyt, P.; Padua, A. A. H. Effect of alkyl chain length and hydroxyl group functionalization on the surface properties of imidazolium ionic liquids. *Phys. Chem. Chem. Phys.* **2011**, *13*, 13518-13526.

(10) Dou, Q.; Sha, M. L.; Fu, H. Y.; Wu, G. Z. Molecular dynamics simulation of the interfacial structure of [C n mim][PF 6] adsorbed on a graphite surface: effects of temperature and alkyl chain length. *J. Physics.: Condens. Matter* **2011**, *23*, 175001.

(11) Hayes, R.; Borisenko, N.; Tam, M. K.; Howlett, P. C.; Endres, F.; Atkin, R. Double Layer Structure of Ionic Liquids at the Au(111) Electrode Interface: An Atomic Force Microscopy Investigation. *J Phys Chem C* **2011**, *115*, 6855-6863.

(12) Mezger, M.; Schramm, S.; Schröder, H.; Reichert, H.; Deutsch, M.; De Souza, E. J.; Okasinski, J. S.; Ocko, B. M.; Honkimäki, V.; Dosch, H. Layering of [BMIM]+-based ionic liquids at a charged sapphire interface. *J Chem Phys* **2009**, *131*, 094701.

(13) Mezger, M.; Schröder, H.; Reichert, H.; Schramm, S.; Okasinski, J. S.; Schöder, S.; Honkimäki, V.; Deutsch, M.; Ocko, B. M.; Ralston, J.; Rohwerder, M.; Stratmann, M.; Dosch, H. Molecular Layering of Fluorinated Ionic Liquids at a Charged Sapphire (0001) Surface. *Science* **2008**, *322*, 424-428.

(14) Elbourne, A.; Voitchovsky, K.; Warr, G. G.; Atkin, R. Ion structure controls ionic liquid near-surface and interfacial nanostructure. *Chemical Science* **2015**, *6*, 527-536.

(15) Segura, J. J.; Elbourne, A.; Wanless, E. J.; Warr, G. G.; Voitchovsky, K.; Atkin, R. Adsorbed and near surface structure of ionic liquids at a solid interface. *Phys Chem Chem Phys* **2013**, *15*, 3320-3328.

(16) Wydro, M. J.; Warr, G. G.; Atkin, R. Amplitude-Modulated Atomic Force Microscopy Reveals the Near Surface Nanostructure of Surfactant Sponge (L3) and Lamellar (Lα) Phases. *Langmuir* **2015**, *31*, 5513-5520.

(17) Buchner, F.; Forster-Tonigold, K.; Uhl, B.; Alwast, D.; Wagner, N.; Farkhondeh, H.; Groß, A.; Behm, R. J. Toward the Microscopic Identification of Anions and Cations at the Ionic Liquid|Ag(111) Interface: A Combined Experimental and Theoretical Investigation. *ACS Nano* **2013**, *7*, 7773-7784.

(18) Li, H.; Su, L.; Zhu, X.; Cheng, X.; Yang, K.; Yang, G. In Situ Crystallization of Ionic Liquid [Emim][PF6] from Methanol Solution under High Pressure. *J Phys Chem B* **2014**, *118*, 8684-8690.

(19) Bovio, S.; Podestà, A.; Lenardi, C.; Milani, P. Evidence of Extended Solidlike Layering in [Bmim][NTf2] Ionic Liquid Thin Films at Room-Temperature. *J Phys Chem B* **2009**, *113*, 6600-6603.

(20) Yokota, Y.; Harada, T.; Fukui, K.-i. Direct observation of layered structures at ionic liquid/solid interfaces by using frequency-modulation atomic force microscopy. *Chemical Comm* **2010**, *46*, 8627-8629.

(21) Grenoble, Z.; Baldelli, S. Ionic Liquids at the Gas-Liquid and Solid-Liquid Interface - Characterization and Properties. *Supported Ionic Liquids: Fundamentals and Applications* **2014**, 145-175.

(22) Xu, S. Y.; Xing, S. R.; Pei, S. S.; Ivanistsev, V.; Lynden-Bell, R.; Baldelli, S. Molecular Response of 1-Butyl-3-Methylimidazolium Dicyanamide Ionic Liquid at the Graphene Electrode Interface Investigated by Sum Frequency Generation Spectroscopy and Molecular Dynamics Simulations. *J Phys Chem C* **2015**, *119*, 26009-26019.

(23) Martinez, I. S.; Baldelli, S. On the Arrangement of Ions in Imidazolium-Based Room Temperature Ionic Liquids at the Gas-Liquid Interface, Using Sum Frequency Generation, Surface Potential, and Surface Tension Measurements. *J Phys Chem C* **2010**, *114*, 11564-11575.

(24) Santos, C. S.; Baldelli, S. Gas-liquid interface of room-temperature ionic liquids. *Chem Soc Rev* **2010**, *39*, 2136-2145.

(25) Santos, C. S.; Rivera-Rubero, S.; Dibrov, S.; Baldelli, S. Ions at the surface of a room-temperature ionic liquid. *J Phys Chem C* **2007**, *111*, 7682-7691.

(26) Paredes, X.; Fernández, J.; Pádua, A. A. H.; Malfreyt, P.; Malberg, F.; Kirchner, B.; Pensado, A. S. Bulk and Liquid–Vapor Interface of Pyrrolidinium-Based Ionic Liquids: A Molecular Simulation Study. *J Phys Chem B* **2014**, *118*, 731-742.

(27) Yan, T.; Li, S.; Jiang, W.; Gao, X.; Xiang, B.; Voth, G. A. Structure of the Liquid−Vacuum Interface of Room-Temperature Ionic Liquids: A Molecular Dynamics Study. *J Phys Chem B* **2006**, *110*, 1800-1806.

(28) Lynden-Bell, R. M.; Del Pópolo, M. G.; Youngs, T. G. A.; Kohanoff, J.; Hanke, C. G.; Harper, J. B.; Pinilla, C. C. Simulations of Ionic Liquids, Solutions, and Surfaces. *Accounts of Chemical Research* **2007**, *40*, 1138-1145.

(29) Shimizu, K.; Pensado, A.; Malfreyt, P.; Padua, A. A. H.; Lopes, J. N. C. 2D or not 2D: Structural and charge ordering at the solid-liquid interface of the 1-(2-hydroxyethyl)-3-methylimidazolium tetrafluoroborate ionic liquid. *Faraday Discuss* **2012**, *154*, 155-169.

(30) Mezger, M.; Roth, R.; Schroder, H.; Reichert, P.; Pontoni, D.; Reichert, H. Solid-liquid interfaces of ionic liquid solutions-Interfacial layering and bulk correlations. *J Chem Phys* **2015**, *142*.

(31) Mezger, M.; Ocko, B. M.; Reichert, H.; Deutsch, M. Surface layering and melting in an ionic liquid studied by resonant soft X-ray reflectivity. *P Natl Acad Sci USA* **2013**, *110*, 3733-3737.

(32) Greaves, T. L.; Drummond, C. J. Protic Ionic Liquids: Evolving Structure-Property Relationships and Expanding Applications. *Chem Rev* **2015**, *115*, 11379-11448.

(33) Merlet, C.; Rotenberg, B.; Madden, P. A.; Salanne, M. Computer simulations of ionic liquids at electrochemical interfaces. *Phys Chem Chem Phys* **2013**, *15*, 15781-15792.

(34) Rotenberg, B.; Salanne, M. Structural Transitions at Ionic Liquid Interfaces. *J Phys Chem Lett* **2015**, *6*, 4978-4985.

(35) Jurado, L. A.; Kim, H.; Arcifa, A.; Rossi, A.; Leal, C.; Spencer, N. D.; Espinosa-Marzal, R. M. Irreversible structural change of a dry ionic liquid under nanoconfinement. *Phys Chem Chem Phys* **2015**, *17*, 13613-13624.

(36) Anaredy, R. S.; Shaw, S. K. Long-Range Ordering of Ionic Liquid Fluid Films. *Langmuir* **2016**, *32*, 5147-5154.

(37) Parr, D.; Chrestenson, J.; Malik, K.; Molter, M.; Zibart, C.; Egan, B.; Haverhals, L. M. Structure and Dynamics at Ionic Liquid/Electrode Interfaces. *ECS Transactions* **2015**, *66*, 35-42.

(38) Lovelock, K. R.; Kolbeck, C.; Cremer, T.; Paape, N.; Schulz, P. S.; Wasserscheid, P.; Maier, F.; Steinruck, H. P. Influence of different substituents on the surface composition of ionic liquids studied using ARXPS. *J Phys Chem B* **2009**, *113*, 2854-2864.

(39) Kolbeck, C.; Cremer, T.; Lovelock, K. R.; Paape, N.; Schulz, P. S.; Wasserscheid, P.; Maier, F.; Steinruck, H. P. Influence of different anions on the surface composition of ionic liquids studied using ARXPS. *J Phys Chem B* **2009**, *113*, 8682-8688.

(40) Lovelock, K. R.; Villar-Garcia, I. J.; Maier, F.; Steinruck, H. P.; Licence, P. Photoelectron spectroscopy of ionic liquid-based interfaces. *Chem Rev* **2010**, *110*, 5158-5190.

(41) Lockett, V.; Sedev, R.; Bassell, C.; Ralston, J. Angle-resolved X-ray photoelectron spectroscopy of the surface of imidazolium ionic liquids. *Phys Chem Chem Phys* **2008**, *10*, 1330-1335.

(42) Kolbeck, C.; Killian, M.; Maier, F.; Paape, N.; Wasserscheid, P.; Steinruck, H. P. Surface characterization of functionalized imidazolium-based ionic liquids. *Langmuir* **2008**, *24*, 9500-9507.

(43) Maier, F.; Cremer, T.; Kolbeck, C.; Lovelock, K. R.; Paape, N.; Schulz, P. S.; Wasserscheid, P.; Steinruck, H. P. Insights into the surface composition and enrichment effects of ionic liquids and ionic liquid mixtures. *Phys Chem Chem Phys* **2010**, *12*, 1905-1915.

(44) Cremer, T.; Stark, M.; Deyko, A.; Steinruck, H. P.; Maier, F. Liquid/solid interface of ultrathin ionic liquid films: [C1C1Im][Tf2N] and [C8C1Im][Tf2N] on Au(111). *Langmuir* **2011**, *27*, 3662-3671.

(45) Hammer, T.; Reichelt, M.; Morgner, H. Influence of the aliphatic chain length of imidazolium based ionic liquids on the surface structure. *Phys Chem Chem Phys* **2010**, *12*, 11070-11080.

(46) Cremer, T.; Wibmer, L.; Calderon, S. K.; Deyko, A.; Maier, F.; Steinruck, H. P. Interfaces of ionic liquids and transition metal surfaces-adsorption, growth, and thermal reactions of ultrathin [C1C1Im][Tf2N] films on metallic and oxidised Ni(111) surfaces. *Phys Chem Chem Phys* **2012**, *14*, 5153-5163.

(47) Hettige, J. J.; Araque, J. C.; Margulis, C. J. Bicontinuity and Multiple Length Scale Ordering in Triphilic Hydrogen-Bonding Ionic Liquids. *J Phys Chem B* **2014**, *118*, 12706-12716.

(48) Hayes, R.; Imberti, S.; Warr, G. G.; Atkin, R. Pronounced sponge-like nanostructure in propylammonium nitrate. *Phys. Chem. Chem. Phys.* **2011**, *13*, 13544-13551.

(49) Hayes, R.; Imberti, S.; Warr, G. G.; Atkin, R. Amphiphilicity determines nanostructure in protic ionic liquids. *Phys. Chem. Chem. Phys.* **2011**, *13*, 3237-3247.

(50) Hayes, R.; Imberti, S.; Warr, G. G.; Atkin, R. Effect of Cation Alkyl Chain Length and Anion Type on Protic Ionic Liquid Nanostructure. *J Phys Chem C* **2014**, *118*, 13998-14008.

(51) Araque, J. C.; Hettige, J. J.; Margulis, C. J. Modern Room Temperature Ionic Liquids, a Simple Guide to Understanding Their Structure and How It May Relate to Dynamics. *J Phys Chem B* **2015**, *119*, 12727-12740.

(52) Kashyap, H. K.; Santos, C. S.; Murthy, N. S.; Hettige, J. J.; Kerr, K.; Ramati, S.; Gwon, J.; Gohdo, M.; Lall-Ramnarine, S. I.; Wishart, J. F.; Margulis, C. J.; Castner, Jr., E. W. Structure of 1-Alky1-1-methylpyrrolidinium Bis(trifluoromethylsulfonyl)amide Ionic Liquids with Linear, Branched, and Cyclic Alkyl Groups. *J Phys Chem B* **2013**, *117*, 15328-15337.

(53) Hettige, J. J.; Kashyap, H. K.; Annapureddy, H. V. R.; Margulis, C. J. Anions, the Reporters of Structure in Ionic Liquids. *J Phys Chem Lett* **2013**, *4*, 105-110.

(54) Kashyap, H. K.; Hettige, J. J.; Annapureddy, H. V. R.; Margulis, C. J. SAXS anti-peaks reveal the length-scales of dual positive-negative and polar-apolar ordering in room-temperature ionic liquids. *Chemical Commun.* **2012**, *48*, 5103-5105.

(55) Kashyap, H. K.; Santos, C. S.; Annapureddy, H. V. R.; Murthy, N. S.; Margulis, C. J.; Castner, Jr., E. W. Temperature-dependent structure of ionic liquids: X-ray scattering and simulations. *Faraday Discuss* **2012**, *154*, 133-143.

(56) Kashyap, H. K.; Margulis, C. J. Theoretical Deconstruction of the X-ray Structure Function Exposes Polarity Alternations in Room Temperature Ionic Liquids. *Molten Salts and Ionic Liquids 18* **2012**, *50*, 301-307.

(57) Annapureddy, H. V. R.; Kashyap, H. K.; De Biase, P. M.; Margulis, C. J. What is the Origin of the Prepeak in the X-ray Scattering of Imidazolium-Based Room-Temperature Ionic Liquids? (vol 114, pg 16838, 2010). *J Phys Chem B* **2011**, *115*, 9507-9508.

(58) Annapureddy, H. V. R.; Kashyap, H. K.; De Biase, P. M.; Margulis, C. J. What is the Origin of the Prepeak in the X-ray Scattering of Imidazolium-Based Room-Temperature Ionic Liquids? *J Phys Chem B* **2010**, *114*, 16838-16846.

(59) Kashyap, H. K.; Margulis, C. J. Theoretical Deconstruction of the X-ray Structure Function Exposes Polarity Alternations in Room Temperature Ionic Liquids. *ECS Trans.* **2013**, *50(11)*, 301-307.

(60) Hettige, J. J.; Araque, J. C.; Kashyap, H. K.; Margulis, C. J. Communication: Nanoscale structure of tetradecyltrihexylphosphonium based ionic liquids. *J Chem Phys* **2016**, *144*.

(61) Hettige, J. J.; Kashyap, H. K.; Margulis, C. J. Communication: Anomalous temperature dependence of the intermediate range order in phosphonium ionic liquids. *J Chem Phys* **2014**, *140*.

(62) Hess, B.; Kutzner, C.; van der Spoel, D.; Lindahl, E. GROMACS 4: Algorithms for highly efficient, load-balanced, and scalable molecular simulation. *J Chem Theory Comput* **2008**, *4*, 435-447.

(63) Van der Spoel, D.; Lindahl, E.; Hess, B.; Groenhof, G.; Mark, A. E.; Berendsen, H. J. C. GROMACS: Fast, flexible, and free. *J Comput Chem* **2005**, *26*, 1701-1718.

(64) Canongia Lopes, J. N.; Shimizu, K.; Pádua, A. A. H.; Umebayashi, Y.; Fukuda, S.; Fujii, K.; Ishiguro, S. A Tale of Two Ions: The Conformational Landscapes of Bis(trifluoromethanesulfonyl)amide and N,N-Dialkylpyrrolidinium. *J. Phys. Chem. B* **2008**, *112*, 1465-1472.

(65) Jorgensen, W. L.; Maxwell, D. S.; Tirado-Rives, J. Development and Testing of the OPLS All-Atom Force Field on Conformational Energetics and Properties of Organic Liquids. *J. Am. Chem. Soc.* **1996**, *118*, 11225-11236.

(66) Price, M. L. P.; Ostrovsky, D.; Jorgensen, W. L. Gas-phase and liquid-state properties of esters, nitriles, and nitro compounds with the OPLS-AA force field. *J Comput Chem* **2001**, *22*, 1340-1352.

(67) Santos, C. S.; Annapureddy, H. V. R.; Murthy, N. S.; Kashyap, H. K.; Castner, Jr., J. E. W.; Margulis, C. J. Temperature-dependent structure of methyltributylammonium bis(trifluoromethylsulfonyl)amide: X ray scattering and simulations. *J. Chem. Phys.* **2011**, *134*, 064501-064501.

(68) Kashyap, H. K.; Santos, C. S.; Daly, R. P.; Hettige, J. J.; Murthy, N. S.; Shirota, H.; Castner, Jr., E. W.; Margulis, C. J. How Does the Ionic Liquid Organizational Landscape Change when Nonpolar Cationic Alkyl Groups Are Replaced by Polar Isoelectronic Diethers? *J Phys Chem B* **2013**, *117*, 1130-1135.

(69) Nosé, S. A unified formulation of the constant temperature molecular dynamics methods. *J. Chem. Phys.* **1984**, *81*, 511-519.

(70) Nosé, S. A molecular dynamics method for simulations in the canonical ensemble. *Mol. Phys.* **1984**, *52*, 255-268.

(71) Parrinello, M.; Rahman, A. Polymorphic transitions in single crystals: A new molecular dynamics method. *J. Appl. Phys.* **1981**, *52*, 7182-7190.

(72) Darden, T.; York, D.; Pedersen, L. Particle mesh Ewald: An N log(N) method for Ewald sums in large systems. *J. Chem. Phys.* **1993**, *98*, 10089-10092.

(73) Essmann, U.; Perera, L.; Berkowitz, M. L.; Darden, T.; Lee, H.; Pedersen, L. G. A smooth particle mesh Ewald method. *J. Chem. Phys.* **1995**, *103*, 8577-8593.

(74) Yeh, I.-C.; Berkowitz, M. L. Ewald summation for systems with slab geometry. *J. Chem. Phys.* **1999**, *111*, 3155-3162.

(75) Yeh, I.-C.; Wallqvist, A. On the proper calculation of electrostatic interactions in solid-supported bilayer systems. *J. Chem. Phys.* **2011**, *134*, 055109-055109.